Thin Solid Films 531 (2013) 160–171

Contents lists available at SciVerse ScienceDirect

Thin Solid Films

journal homepage: www.elsevier.com/locate/tsf

Comparative studies of laser annealing technique and furnace annealing by X-ray diffraction and Raman analysis of lithium manganese oxide thin films for lithium-ion batteries

J. Pröll [a,*], P.G. Weidler [c], R. Kohler [a], A. Mangang [a], S. Heißler [c], H.J. Seifert [a], W. Pfleging [a,b]

[a] Karlsruhe Institute of Technology, Institute for Applied Materials (IAM-AWP), P.O. Box 3640, 76021 Karlsruhe, Germany
[b] Karlsruhe Nano Micro Facility, H.-von-Helmholtz-Platz 1, 76344 Egg.-Leopoldshafen, Germany
[c] Karlsruhe Institute of Technology, Institute of Functional Interfaces (IFG), P.O. Box 3640, 76021 Karlsruhe, Germany

ARTICLE INFO

Article history:
Received 19 January 2012
Received in revised form 11 January 2013
Accepted 11 January 2013
Available online 17 January 2013

Keywords:
Laser annealing
Furnace annealing
Raman spectroscopy
X-ray diffraction
Thin films
Lithium-ion batteries
Lithium manganese oxide
Spinel phase

ABSTRACT

The structure and phase formations of radio frequency magnetron sputtered lithium manganese oxide thin films ($Li_{1.1}Mn_{1.9}O_4$) under ambient air were studied. The influence of laser annealing and furnace annealing, respectively, on the bulk structure and surface phases was compared by using ex-situ X-ray diffraction and Raman analysis. Laser annealing technique formed a dominant (440)-reflection, furnace annealing led to both, (111)- and (440)-reflections within a cubic symmetry (S.G. Fd3m (227)). Additionally, in-situ Raman and in-situ X-ray diffraction were applied for online detection of phase transformation temperatures. In-situ X-ray diffraction measurements clearly identified the starting temperature for the (111)- and (440)-reflections around 525 °C and 400 °C, respectively. The 2θ Bragg peak positions of the characteristic (111)- and (440)-reflections were in good agreement with those obtained through conventional furnace annealing. Laser annealing of lithium manganese oxide films provided a quick and efficient technique and delivered a dominant (440)-reflection which showed the expected electrochemical behavior of the well-known two-step de-/intercalation process of lithium-ions into the cubic spinel structure within galvanostatic testing and cyclic voltammetry.

1. Introduction

Currently, secondary lithium-ion cells enclose cathode materials such as layered compounds like $LiCoO_2$, $LiNiO_2$ or $LiMnO_2$, and olivine-type materials like $LiFePO_4$, or spinel-type $LiMn_2O_4$ [1]. Differences can be found in the type of lithium diffusion while the olivine-type provides 1-dimensional [2], the layered compounds 2-dimensional [3] and the spinel-type 3-dimensional diffusion paths [3]. The practical capacities also differ within those materials, counting 140 mAh/g for $LiCoO_2$, 170 mAh/g for $LiFePO_4$ and 110 mAh/g for $LiMn_2O_4$ [1,3]. Typically, spinel $LiMn_2O_4$ is one promising candidate because of its non-toxicity [4], its high operating voltage in the 4 V region [5] and low material costs [6,7]. Within the system of lithium manganese oxides, several promising compounds for use as cathodes are listed in literature such as orthorhombic $LiMnO_2$ [8–10] or cubic spinel $LiMn_2O_4$ [11–14]. Especially, the formation of cubic spinel solid solutions under air is very sensitive to their synthesizing temperatures and the lithium-to-manganese ratio as was already reported by Paulsen and Dahn [15]. Hence, one promising aspect is to study the spinel-type structure formation and development of radio frequency (rf) magnetron sputtered thin films when heating the material with in-situ analytics for obtaining detailed information on the onset of crystallization processes and temperatures. Other in-situ studies were focused on reversible and irreversible transformations of stoichiometric $LiMn_2O_4$ in air [16] or on in-situ X-ray diffraction (XRD) studies during lithium deintercalation from the spinel host structure [17]. rf magnetron sputtering is one promising method for synthesizing thin lithium manganese oxide films which have model character [18–21] and to study clearly their structural behavior due to the absence of carbon and binder as can be found in tape cast electrodes. Rapid laser annealing is one possible technique for crystallization of thin cathodes such as $LiCoO_2$ [22–24] or Li–Mn–O [20,21]. Besides that, other rapid annealing processes for Li–Mn–O thin films have already been applied in the past by using halogen lamps for so-called rapid thermal annealing [25–29]. In this work, laser annealing of rf magnetron sputtered lithium manganese oxide thin films was investigated. The aim was to form a spinel-like phase and to study it by using integral chemical analysis, Raman spectroscopy, X-ray diffraction methods, scanning electron microscopy and electrochemical measurements. Furthermore, the as-deposited films were conventionally furnace annealed and analyzed by Raman and X-ray diffraction techniques as well. In addition to the processes of laser annealing and conventional furnace heating, in-situ analytics were applied in order to obtain more detailed

* Corresponding author.
E-mail addresses: johannes.proell@kit.edu, johannes.proell2@kit.edu (J. Pröll).

0040-6090/$ – see front matter © 2013 Elsevier B.V. All rights reserved.
http://dx.doi.org/10.1016/j.tsf.2013.01.015

information on the onset of phase formation during heating of the thin films.

2. Experimental details

2.1. Thin film deposition

rf magnetron sputtering of lithium manganese oxide thin films was investigated with a Leybold Z550 coating facility. Stainless steel (diameter 12 mm) and silicon (100) (area 10×10 mm^2) substrates were used. They were ultrasonically cleaned in acetone and isopropanol each for 15 min and subsequently plasma-etched in argon for 15 min. The target material was $LiMn_2O_4$ (99.9%, MaTeck GmbH) with a diameter of 7.6 cm and a thickness of 0.6 cm. The target–substrate plate distance was 6 cm. Film deposition was carried out with a target power of 200 W and a working gas pressure of 0.25 Pa argon. An Au buffer layer of about ~100 nm was also deposited in between the substrate and the Li–Mn–O film. The film thickness was determined with a surface profilometer (Tencor P-10) and counted 2–3.3 μm depending on the position of the substrate on the plate. The density of an as-deposited Li–Mn–O thin film with a thickness of about ~67 nm was measured to be about 4 g/cm^3 via X-ray reflectivity [21] and was considered for calculation of the active mass for electrochemical cycling of laser annealed thin films assuming that no mass losses occur [30] during the annealing process at temperatures of T = 680 °C.

2.2. Laser annealing and conventional furnace heating

Laser annealing was investigated with a high power diode laser system (FLS IronScan, Fisba Optik AG) operating at a wavelength of λ = 940 nm. The laser beam had a focus diameter of 1 mm. The temperature was online-controlled by a pyrometer (FLS PyroS, Fisba Optik AG) and the adjustment time was 1 ms. Temperature control was possible in the range of 120–700 °C. The laser beam was scanned over the sample surface via deflection mirrors with a laser scanning velocity of 1000 mm/s for all experiments. A schematic description of the laser annealing process is given in Fig. 1. The laser beam was scanned over the sample surface in eight different directions marked by positions 1–8 (Fig. 1) in order to achieve a homogeneous heating of the sample. One scanning step—including positions 1–8—took about 2.7 s. This scanning strategy was repeated in order to achieve overall annealing times of 100 s as well as 2000 s, respectively.

Furnace annealing of the samples was performed via a tube furnace (Gero Hot Solutions) using heating and cooling rates of 300 K/h. The two annealing temperatures of T = 600 °C as well as T = 700 °C were held, each for 3 h. The processing gas was ambient air for furnace and laser annealing.

2.3. Raman and XRD

Micro-Raman spectroscopy was applied for phase identification after laser and furnace annealing of the films. A Renishaw-1000 system equipped with an argon laser, operating with an excitation wavelength of λ_{Raman} = 514.5 nm and a 50× objective was used. The output power was 2.3 mW for all measurements in order to avoid phase changes during measurement. In-situ as well as ex-situ Raman spectroscopy was also performed using a Senterra Raman spectrometer (Bruker Optics GmbH) operating with a frequency doubled DPSS Nd:YAG laser at a wavelength of 532 nm. The power during the measurements was set to 10 mW and a 50× MPLAN Olympus objective (Olympus, Tokyo Japan) was used. For sample heating during in-situ Raman analysis, a Linkam high temperature system was used consisting of the heating stage (type TS1500, maximal temperature 1500 °C) and a T95-LinkPad controller (Linkam Scientific Instruments, Guildford, UK). The specimen was placed inside the ceramic sample cup so that it could be heated from underneath as well as from the sides. A ceramic heat shield was placed over the top to prevent heat loss. The samples were heated up to T = 900 °C with a constant heating rate of 600 K/h. In order to investigate the in-situ Raman measurements during heating, defined temperatures were stabilized, each by the controller unit for t = 300 s, respectively. Raman bands were assigned by fitting the recorded spectra with Lorentz function.

Information on the crystalline phases of laser and furnace annealed films was obtained by X-ray diffraction (type Seifert PAD II, Bragg-Brentano arrangement, Cu $K_{\alpha1}$ radiation, λ_{XRD} = 0.15406 nm). In-situ X-ray diffraction analysis was carried out by using a diffractometer of the type Bruker D8 Advance (Bruker AXS, Karlsruhe, Germany) and an HTK 1200 (Anton Paar, Graz, Austria) heating unit. The samples were heated with a 600 K/h heating rate. Diffractograms were recorded over an angular range from 10° 2θ to 90° 2θ with 0.02° 2θ step width and counting rate of 0.4 s per step with Cu $K_{\alpha1,2}$ radiation. A Lynxeye PSD detector shortened the overall measurement time drastically still providing long counting times for each step. The divergence slit was fixed at 0.4 mm. Simulation of XRD patterns was done with help of the Bruker AXS Rietveld software TOPAS applying structure files obtained from the American Mineralogist Crystal Structure Database [31–33].

2.4. Reference powder

Lithium manganese oxide powder ($Li_{1+x}Mn_{2-x}O_4$ where x = 0.0–0.2, MTI Corporation)—further named in the text as spinel

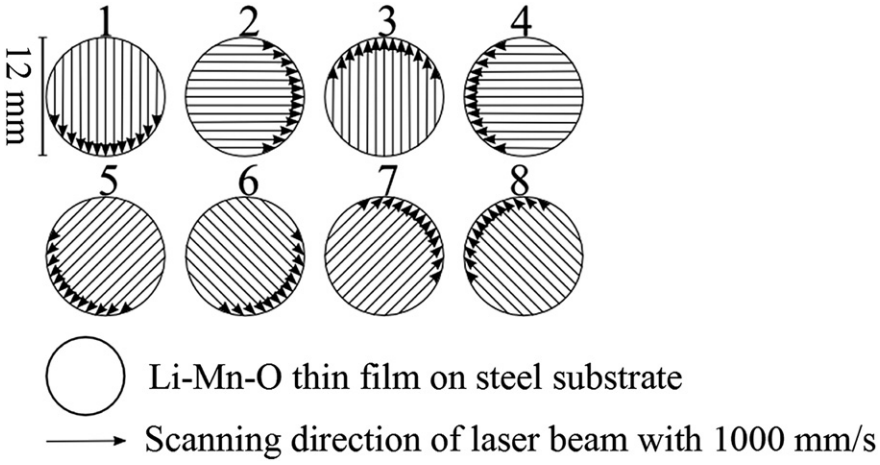

Fig. 1. Schematic view of the laser annealing process for Li–Mn–O thin films on stainless steel substrates. The scanning strategy (positions 1–8) is shown.